2019 16th International Conference on Electrical Engineering, Computing Science and Automatic Control (CCE), Mexico City, Mexico. September 11-13, 2019

# Procedure for Removing Artifacts from EMG Signals Envelope Assuming CMN

Sandra Márquez-Figueroa, Yuriy S. Shmaliy, Oscar Ibarra-Manzano,Carlos Lastre-Domínguez, Miguel Vazquez-Olguin
Department of Electronics Engineering
Universidad de Guanajuato
Salamanca, 36885, México
Email: {s.marquezifigueroa} {shmaliy} {ibarrao}{cm.lastredominguez} {miguel.vazquez}@ugto.mx

***Abstract*—The estimation of the envelope is an important issue in surface electromyography (EMG) signal processing, which has relevant applications. The present document shows the process of getting the best envelope from the EMG signals based on digital filtering, the following algorithms have been implemented: the discrete-time state-space unbiased finite impulse response (UFIR) filter, Kalman filter (KF), and algorithms in discrete-time state-space for Gauss-Markov CMN such as cUFIR and cKF. We exploit EMG records of the electrical activity of muscles during movement. The motion for a resolution we tabled shows that better smoothing can be obtained using cUFIR and cKF. Higher accuracy of the developed cUFIR and cKF algorithms against UFIR and KF is demonstrated experimentally and by simulation.**

## I. Introduction

Electromyography (EMG) signals are laid out rather noisy with rapid and random changes [1]. These signals represent the muscle movement generated by electrical activity in response to nerve stimulation [2] and features of the EMG waveform depend on the geometric position of the inserted needle electrode in the muscle. We should regard these indisputable signals are complex to analyze, given that MUAPs are acquired by electrodes from various areas of the motor unit (MU). Furthermore, a skeletal muscle has hundreds of different muscle fiber types, and the resulting signal is composed of several MUAPs [2]–[7].

EMG signals are contaminated by sensor noise and artifacts that originate from different sources, such as electrocardiogram interference, spurious background spikes and, motion artifacts [2], [8]. Rapid changes generated by noise affect EMG data, consequently, EMG signal processing requires special algorithms for noise extraction with high accuracy. Many solutions have been developed to extract the characteristics of the EMG signal and analyze the behavior of MU for different applications, such as bioelectronics, robotic, and biomedical applications. Features extraction from the EMG signal measurements is required for medical needs to detect different diseases and recognize muscle state more easily. [2], [9].

Linear envelope (LE) signals can be produced by the Hilbert transform [10], mean square error (MSE) criterion [11], and waveform produced [12]. The envelope of the EMG signal is used in robotic systems and prothesis control to achieve a perfect collaboration between man and robot [13], [14].

Researchers often apply several techniques designed to acquire the envelope of the EMG signal, such as the reflective envelope of the activity of the moving average [15], low pass filtering with a Butterworth filter, single pass, cutoff frequency of 3Hz [16], but It has been shown that it may produce unacceptably large bias errors and does not avoid spikes. Better results are achieved employing the Savitsky-Golay smoother combined with a low-pass filter [17]. Smoothing provides better envelope shaping, but introduces time-delay-lags, which may not be tolerated in robotic schemes.

In [13], [18], the EMG signal envelope has been extracted taking advantage of time-frequency analysis via the EMG signal energy on given finite time windows. Another way is to rectify the surface EMG prior to subsequent coherence analysis [19]. The rectification often effectively enhances the firing rate information of the signal, but typically does not avoid problems with high envelope variability [20].

Optimal Kalman filter (KF) algorithm setting allows achieving a maximum estimation accuracy, noise is required to be white Gaussian with known statistics. Kalman filter may not be effective in EMG data analysis unless certain requirements are satisfied. Therefore no essential advantage was demonstrated against other available methods. The unbiased finite impulse response (UFIR) filter [21], which completely ignores zero mean noise, is considered as a robust alternative to the KF [22] and can also be applied to suppress EMG noise.

### A. Features of EMG Signals

The morphology of a muscle is fundamental for extracting features of EMG signals. The records of the changes produced in the muscles of the MU (motor unit) are known as AP (action potential) [23]. Under normal conditions, The EMG signal $u(t)$ voltage typically ranges as $\pm 5\,\mathrm{mV}$ prior to amplification [2], the duration of the UM varies between 8 and 14 $ms$ according to the size [23]. A suggested sampling frequency $f = 2\,\mathrm{kHz}$ [24] corresponds to a sampling time of $\tau = 0.5\,\mathrm{ms}$, although $f$ may range as $(0.25 \ldots 3)\,\mathrm{Hz}$ [25]. A spectral peak of the EMG signal is typically found at $(60 \ldots 100)\,\mathrm{Hz}$.

978-1-5386-7033-0/18/$31.00 

Features of the waveform of the AP depend on certain structural and functional dimensions of the MU. Neurogenic and myopathic pathological processes can alter these dimensions, which are expressed by abnormal deviations of the parameters of the AP [23].

## II. Removing Artifacts of EMG Signal Envelope

### A. EMG Signal Envelope

Issues associated with the EMG signal envelope extraction and shaping can be considered following Fig. 1.

The envelope of $u(t)$ will be given by $u(k)$ and is often referred to as the instantaneous amplitude. Digital version $u_k$ of the EMG signal may thus be highly oversampled in the discrete time index $k$ corresponding to time $t_k$ and $\tau = t_n - t_{k-1}$.

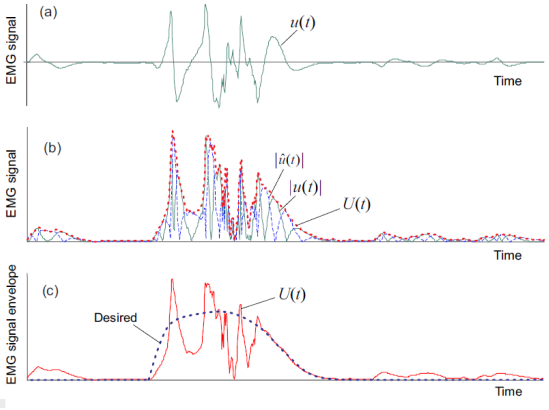


Fig. 1. EMG signal envelope in an the EMG signal available from [26]: (a) measured EMG signal $u(t)$, (b) Hilbert transform $\hat{u}(t)$ of $u(t)$ and envelope $U(t) = \sqrt{u^2(t) + \hat{u}^2(t)}$, and (c) extracted $U(t)$ and desired EMG signal envelope.

If the fiber-generated MUAP density is low, an effective envelope extraction technique may be achieved via the Hilbert transform, $\hat{u}_n$ of $u_k$ can be used to draw the envelope $U_k = \sqrt{u_k^2 + \hat{u}_k^2}$, therefore, $u(k) \geq \mid u_k(t) \mid$. Otherwise, if the MUAP density is high and the envelope edges are sharp, the Hilbert transform is not used.

We now emphasize on two specifics of the EMG signal envelope:

- The oversampled parts of $U_k$ can be approximated with order $K$ polynomials.
- Envelope $U_k$ is commonly highly disturbed by multiple excursions and cannot be used efficiently in robotics and control systems.

### B. State-Space Model of EMG Signal Envelope

Let us represent the envelope $U_n$ in discrete-time index $n$ with the $K$-state-space polynomial model [27] assuming Gauss-Markov CMN $v_n$ as

$$x_n = A_n x_{n-1} + B_n w_n \,, \tag{1}$$

$$y_n = H_n x_n + v_n \,, \tag{2}$$

$$v_n = \psi_n v_{n-1} + \xi_n \,, \tag{3}$$

where $x_n \in \mathbb{R}^k$ is the $U_n$ state vector and $y_n$ is the scalar observation of $U_n$. For polynomial approximation, entries of the system matrix $A_n$ are provided by the Taylor series [27], [28],

$$A_n = \begin{bmatrix} 1 & \tau & \frac{\tau^2}{2} & \dots & \frac{\tau^{K-1}}{(K-1)!} \\ 0 & 1 & \tau & \dots & \frac{\tau^{K-2}}{(K-2)!} \\ 0 & 0 & 1 & \dots & \frac{\tau^{K-3}}{(K-3)!} \\ \vdots & \vdots & \vdots & \ddots & \vdots \\ 0 & 0 & 0 & \dots & 1 \end{bmatrix} \tag{4}$$

and we notice that the number $K \triangleq K_n$ of the states can be different at each time index $n$ to achieve the best filtering effect; that is, $A_n$ is generally time-varying. Observation $y_n$ of $U_n$ corresponds to the first state. Therefore, the observation matrix $H_n = [\,1\ 0 \dots 0\,] \in \mathbb{R}^{1\times k}$ may also be time-varying for $K_n$. Matrix $B_n \in \mathbb{R}^{k\times P}$ projects $U_n$ noise $w_n \in \mathbb{R}^P$ to $x_n$. The scalar color factor $\psi_n$ is supposed to be known at each $n$ and such that noise $v_n$ is stationary; by $\psi_n = 0$, noise $v_n$ is supposed to be white, as required by optimal estimators.

Because the $U_n$ noise $w_n$ is generally unknown, we will suppose that it has zero mean with uncertain both the statistics and distribution. However, to run the KF, we will consider $w_n$ as zero mean and white Gaussian, $w_n \sim \mathcal{N}(0, Q_n) \in \mathbb{R}^P$, with the covariance $E\{w_n w_k^T\} = Q_n \delta_{n-k}$, where $\delta_n$ is a Kroneker symbol, which has unknown entries. Noise $\xi_n$ is zero mean and white Gaussian, $\xi_n \sim \mathcal{N}(0, \sigma_n^2)$, with the variance $E\{\xi_n^2\} = R_n = \sigma_{\xi n}^2$ and the property $E\{w_n \xi_k\} = 0$ for all $n$ and $k$.

We assume that the estimate $\hat{x}_n \triangleq \hat{x}_{n|n}$ of $x_n$ under the intensive non white variations in $U_n$ (Fig. 1c) will range closer to the desired envelope if to suppose the CMN. Therefore, below we will develop two possible linear approaches to shape $U_n$: the KF, which requires all information about the initial values and supposedly white Gaussian noise, and the UFIR filter, which completely ignores these requirements and is thus more robust [22].

## III. Extraction of EMG Signal Envelope under CMN

The known KF algorithms assuming CMN were designed for the predictive state model $x_n = A_n x_{n-1} + B_n w_{n-1}$, which differs from (1) by the past noise term $w_{n-1}$ On the other hand, the UFIR filter was derived in [27] for (1). Therefore, to unify the solutions, we will modify the KF and UFIR algorithms for (1)–(3) and call them accordingly as cKF and cUFIR.

### A. cKF Algorithm

To apply the KF to (1)–(3), one can follow [29], consider a new observation $z_n$ as measurement differences, and write

$$\begin{aligned} z_n &= y_n - \psi_n y_{n-1} \,, \\ &= H_n x_n + v_n - \psi_n H_{n-1} x_{n-1} - \psi_n v_{n-1} \,. \end{aligned} \tag{5}$$

By taking $x_{n-1}$ from (1) and $v_{n-1}$ from (3), a new observation can be written as

$$z_n = D_n x_n + \bar{v}_n \,, \tag{6}$$

where $D_n = H_n - \Gamma_n$, $\Gamma_n = \psi_n H_{n-1} A_n^{-1}$, and

$$\bar{v}_n = \Gamma_n B_n w_n + \xi_n \tag{7}$$

is white Gaussian scalar noise with the properties,

$$\begin{aligned} E\{\bar{v}_n^2\} &= \Gamma_n \Phi_n + R_n = \Gamma_n \Phi_n + \sigma_{\xi n}^2 \,, & (8)\\ E\{\bar{v}_n w_n^T\} &= \Gamma_n B_n Q_n \,, & (9) \end{aligned}$$

where the weighted matrix $Q_n$ is

$$\Phi_n = B_n Q_n B_n^T \Gamma_n^T \,. \tag{10}$$

The modified state-space model (1) and (6) has now time-correlated and white $w_n$ and $\bar{v}_n$ and the KF can be applied, if to derive the optimal bias correction gain taking into account the correlation. For given $y_n$, $\hat{x}_0$, $P_0$, $Q_n$, $R_n$, $\psi_n$, and CMN, the cKF algorithm becomes

$$\begin{aligned} z_n &= y_n - \psi_n y_{n-1} \,, & (11)\\ P_n^- &= A_n P_{n-1} A_n^T + B_n Q_n B_n^T \,, & (12)\\ S_n &= D_n P_n^- D_n^T + R_n + H_n \Phi_n + \Phi_n^T D_n^T \,, & (13)\\ K_n &= (P_n^- D_n^T + \Phi_n) S_n^{-1} \,, & (14)\\ \hat{x}_n^- &= A_n \hat{x}_{n-1} \,, & (15)\\ \hat{x}_n &= \hat{x}_n^- + K_n (z_n - D_n \hat{x}_n^-) \,, & (16)\\ P_n &= (I - K_n D_n) P_n^- - K_n \Phi_n^T & (17) \end{aligned}$$

and, by $\psi_n = 0$ and $\Phi_n = 0$, it becomes the standard KF.

### *B. UFIR Filtering Algorithm*

The UFIR filter [21] can be more suitable for EMS signals, because it does not require any information about noise, except for the zero mean assumption. To provide a near optimal estimate, this filter requires an averaging horizon $[m, n]$ of $N$ points, from $m = n - N + 1$ to $n$, to be optimal $N_{\rm opt}$ in the MSE sense. Of importance is that $w_n$ and $\bar{v}_n$ are both zero mean and their correlation does not produce bias. Therefore, the UFIR filter can be applied directly to (1) and (6), unlike the KF.

The cUFIR algorithm operates as follows. Given $N$, $y_n$, and $\psi_n$, one must set $n = N-1, N, \ldots$, $m = n - N + 1$, and $s = n - N + K$ and compute the initial values $G_s = (C_{m,s}^T C_{m,s})^{-1}$ and $\bar{x}_s = G_s C_{m,s}^T Y_{m,s}$ in short batch forms via $Y_{m,s} = [\, y_m \ \ldots \ y_s \,]^T$ and

$$C_{m,s} = \begin{bmatrix} D_m (A_s ... A_{m+1})^{-1} \\ \vdots \\ D_{s-1} A_s^{-1} \\ D_s \end{bmatrix} . \tag{18}$$

Provided the initial values at $s$, iteratively updated values appear for $l = s+1, \ldots, n$ using the recursions

$$\begin{aligned} z_l &= y_l - \psi_l y_{l-1} \,, & (19)\\ G_l &= [D_l^T D_l + (A_l G_{l-1} A_l^T)^{-1}]^{-1} \,, & (20)\\ K_l &= G_l D_l^T \,, & (21)\\ \bar{x}_l^- &= A_l \bar{x}_{l-1} \,, & (22)\\ \bar{x}_l &= \bar{x}_l^- + K_l (z_l - D_l \bar{x}_l^-) \,, & (23) \end{aligned}$$

and the output estimate $\hat{x}_n = \bar{x}_n$ is taken when $l = n$. It also follows that, by $\psi_n = 0$, the cUFIR algorithm becomes the standard UFIR filter [21].

In the error covariance for the UFIR filter $K_n$ is replaced by $G_n$ and recalled that $G_n$ is symmetric [21]. That yields

$$\begin{aligned} P_n &= (I - G_n D_n^T D_n) P_n^- (I - G_n D_n^T D_n)^T \\ &\quad + G_n D_n^T (\Gamma_n \Phi_n + R_n) D_n G_n \\ &\quad - 2(I - G_n D_n^T D_n) \Phi_n D_n G_n \\ &= P_n^- - 2(P_n^- D_n^T + \Phi_n) D_n G_n + G_n D_n^T S_n D_n G_n \\ &= P_n^- - (2 P_n^- D_n^T + 2\Phi_n + G_n D_n^T S_n) D_n G_n \,, \quad (24) \end{aligned}$$

where $P_n^-$ is given by (12) and $S_n$ by (13). Note that the cUFIR algorithm does not require $P_n$, although the recursion (24) can be included to for any purposes.

## IV. Applications

In this section, we will apply the cKF and cUFIR algorithms to two types of EMG data. First, we will consider EMG signals with low MUAP density, which require the Hilbert transform to shape the envelope. Next, we will process well pronounced EMG signals with high MUAP density and sharp edges, in which case only better denoising of the envelope is required.

For all EMG data, we specify model (1)–(3) with two states, $K = 2$, and matrices

$$A = \begin{bmatrix} 1 & \tau \\ 0 & 1 \end{bmatrix} , B = \begin{bmatrix} \frac{\tau^2}{2} \\ \tau \end{bmatrix} , H = \begin{bmatrix} 1 & 0 \end{bmatrix} .$$

We suppose that the envelope noise $w_k$ acts in the third state and projects to state $x_k$ by matrix $B$

### *A. EMG Signals for Low MUAP Density*

*1) First experiment:* We start with a surface EMG signal database collected for lower limb analysis and available from [30]. The database contains samples from 11 subjects with knee abnormality previously diagnosed by a professional and 11 normal knees. All data are collected using the EMG and goniometry equipment MWX8 Datalog Biometrics. Measurements are provided with the sampling frequency $F = 1\,\text{kHz}$ that corresponds to $\tau = 10^{-3}\,\text{s}$. A part of database "1Amar" observed in a time span of $(2.6 \ldots 3.4)\,\text{s}$ is shown in Fig. 2a. The envelope for low MUAP density was shaped here using the Hilbert transform and sketched in Fig. 2b and Fig. 2c as "data".

No information about noise is provided in [30]. Therefore, we voluntary tune the filters to produce consistent estimates with minimal variations about the desired smooth envelope and insignificant time-delays.

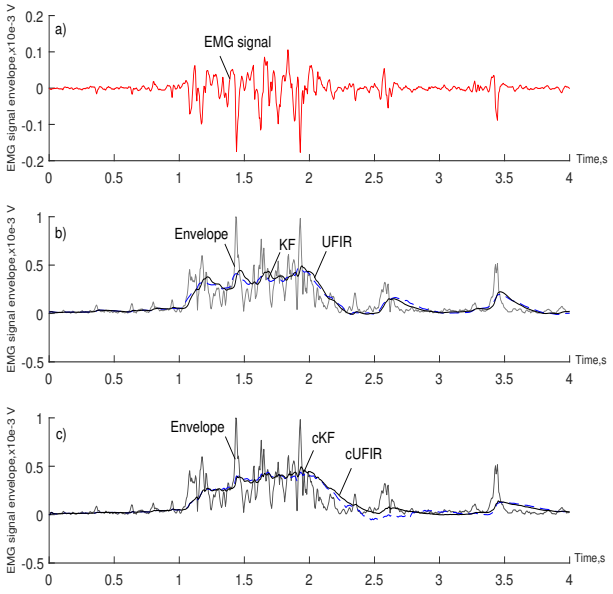


Fig. 2. Envelope extraction for low MUAP density in an EMG signal available from [30]: (a) part of the EMG signal database, (b) envelope obtained using the Hilbert transform and KF and UFIR estimates, and (c) envelope and cKF and cUFIR estimates.

| RMS | | | |
|---|---|---|---|
| KF | UFIR | cKF | cUFIR |
| 0.068001 | 0.066692 | 0.043512 | 0.04421 |

TABLE I
RMS VALUE BETWEEN THE GAUSSIANITY AND ALGORITHMS [31].

For the UFIR filter we have experimentally found $N_{\text{opr}} = 74$, which means that data are highly oversampled. To tune the KF, we supposed that the measurement noise has the standard deviation of $\sigma_\xi = 50\,\mu\text{V}$ and set $\sigma_w = 0.1\,\text{V/s}^2$ for the KF estimate to be consistent to the UFIR estimate. We then run both filters and arrive at estimates shown in Fig. 2b. As can be seen, the envelope is shaped by the filters much better than by the Hilbert transform and there is no essential time-delays, as required. However, the envelope is still corrupted by multiple excursions.

To suppress excursions, we nest tune the cKF and cUFIR algorithms for $\psi = 0.65$ and $\bar{N}_{\text{opt}} = 170$. The results are shown in Fig. 2c. Even a quick look at this figure reveals that excursions are removed from many parts of the envelope, which definitely looks more smoothed.

EMG Gaussianity is a relevant assessment because EMG should exhibit properties of a Gaussian process [32], [33]. The relation between the Gaussianity and the envelope given by the algorithms is illustrated in table I. Based on the data the RMS value is calculated for each algorithm [31], [34], which show that the cUFIR and cKF algorithms have high accuracy.

*2) Second experiment:* In this area, we considered an "aggressive" EMG signal from the database "Elbowing," which is available from [26]. The selected part of a signal shown in Fig. 3a was processed similarly to the first one (Fig. 2) with the same tuning parameters.

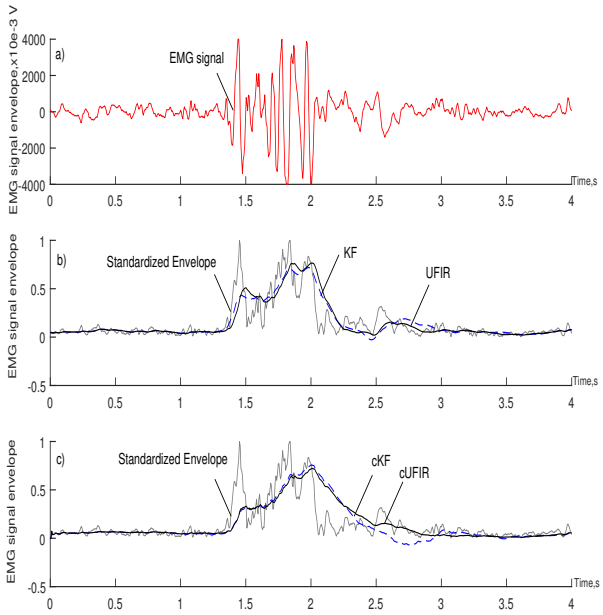


Fig. 3. Envelope extraction for low MUAP density in an EMG signal available from [26]: (a) part of the EMG signal database, (b) standardized envelope (data) obtained using the Hilbert transform and KF and UFIR estimates, and (c) standardized envelope and cKF and cUFIR estimates.

| RMS | | | |
|---|---|---|---|
| KF | UFIR | cKF | cUFIR |
| 0.078999 | 0.060849 | 0.046753 | 0.048381 |

TABLE II
RMS VALUE BETWEEN THE GAUSSIANITY AND ALGORITHMS [31].

As can be concluded, the KF and UFIR filter still produce consistent estimates with no essential time-delays. It can also be seen that the cKF and cUFIR filter better suppress the excursions with $\psi_{\text{opt}} = 0.65$. On a broader timescale, envelopes of several EMG "Elbowing" signals provided using all filters are given in Fig. 4. This figure assures that the interpretation of variations in the EMG signal as Gauss-Markov CMN allows getting better envelope shaping and artifacts removal.

| RMS | | | |
|---|---|---|---|
| KF | UFIR | cKF | cUFIR |
| 0.09304 | 0.088562 | 0.060864 | 0.062515 |

TABLE III
RMS VALUE BETWEEN THE GAUSSIANITY AND ALGORITHMS [31].

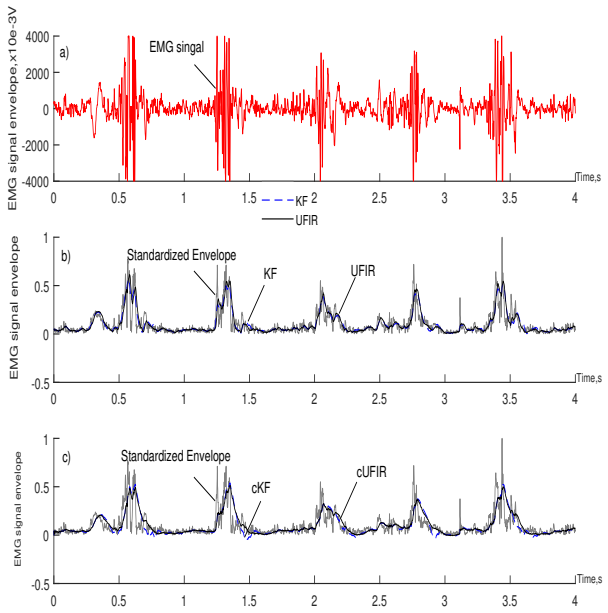


Fig. 4. Envelope extraction for low MUAP density EMG signals on a wider time scale [26]: (a) part of the EMG signal database, (b) standardized envelope (data) obtained using the Hilbert transform and KF and UFIR estimates, and (c) standardized envelope and cKF and cUFIR estimates.

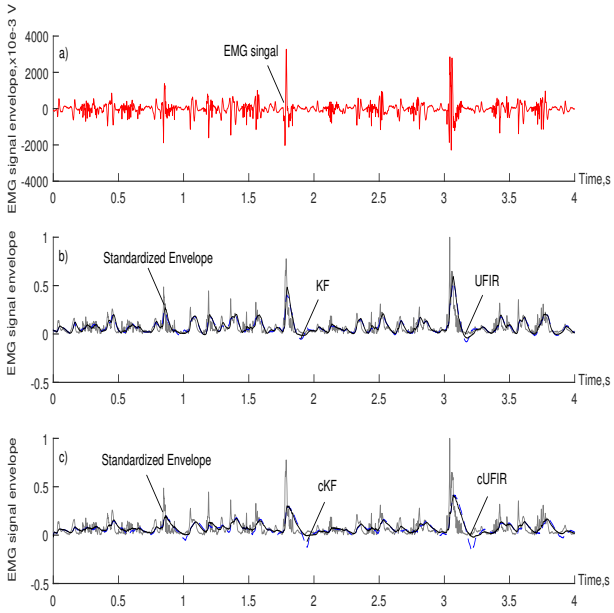


[h]

Fig. 5. Envelope extraction for a high MUAP density EMG signal with sharp edges available from [35]: (a) absolute measured EMG signal, (b) KF and UFIR filter estimates, and (c) cKF and cUFIR filter estimates.

Two main conclusions can be made by observing this figure:

- The color factor $\psi$ must be optimized for the best desirable envelope shape,
- Factor $\psi$ should not exceed 1.0, because $v_n$ does not obey the requirement of stationarity otherwise.

The results in tables II and III clearly show the RMS value of the EMG signals in Figures 3 and 4 respectively, indicating the same result of the table I.

### *B. EMG Signals for High MUAP Density with Sharp Edges*

Finally, we consider several well-pronounced EMG signals with high MUAP densities and sharp edges, which absolute values sampled with $F = 2\,\text{kHz}$ and $\tau = 0.1\,\text{ms}$ are available from [35]. From this database, we select two types of EMG signals represented with 1) impulse sequences (Fig. 5a) and 2) continuously generated MUAPs. We do not apply the Hilbert transform in this case and tune the filters for $\sigma_w = 0.3\,\text{V/s}^2$, $\sigma_\xi = 50\,\mu\text{V}$, $N_{\text{opt}} = 170$, and $\bar{N}_{\text{opt}} = 110$.

A specific is that, for high MUAP density, the envelope noise becomes more like white rather than colored, although it is still definitely not white. This observation means that the color factor $\psi$ should be smaller than in the above considered cases. Furthermore, because the colored noise is less pronounced, one should expect lesser effects from the cKF and cUFIR filter that will be illustrated below.

*1) EMG Impulse Sequences with Sharp Edges:* The envelopes shaped by the KF and UFIR filter for an EMG impulse sequence with sharp edges shown in Fig. 5a are sketched in Fig. 5b and one infers that there is not big difference between the estimates.

| RMS | | | |
|---|---|---|---|
| KF | UFIR | cKF | cUFIR |
| 0.055205 | 0.60952 | 0.041035 | 0.038852 |

TABLE IV
RMS VALUE BETWEEN THE GAUSSIANITY AND ALGORITHMS [31].

Aimed at providing better shaping, the cKF and cUFIR filter are next applied with the color factor $\psi_{\text{opt}} = 0.6$ to produce the envelopes shown in Fig. 5c. Note is that the value of $\psi$ is smaller than in the above cases, as expected.

Although the color noise in Fig. 5a is not as large as in the previous case (Fig. 2), the cKF and cUFIR filter still improve the envelope smoothness and suppress some artifacts. This is especially neatly seen in the last fifth impulse in Fig. 5, in which case the envelope is better shaped and two small artifacts in Fig. 5b are well suppressed in Fig. 5c. The RMS value is shown in table IV.

## V. CONCLUSIONS

In this paper, we realized a study about applications of the UFIR filter, cUFIR filter, KF algorithm , and cKF algorithm in the state space to give denoising of EMG signal envelope. These results can be considered for medical robotic applications as an alternative solution in the decision making for medical diagnosis and control systems.

As has been seen from various outcomes that algorithms developed in this paper assuming CMN in the envelope have demonstrated better performance than the standard solutions. The effect was achieved by suppressing the color noise-like variations and artifacts in the envelope with no essential time delays. Based upon extensive investigations, we suggest that the cKF should be used when a sufficient information is available about noise. Otherwise, one should apply the cUFIR filter, which ignores zero mean noise and is thus more robust against errors in the noise statistics.

Experimental verification provided based on different EMG signals have shown that the cKF and cUFIR algorithms are efficient when the MUAP density is low, in which case intensive excursions in the envelope are reminiscent of the colored noise. Shaped with high a MUAP density, the envelope typically demonstrates smaller variations and the filters designed become less efficient. In both cases, the color factor must be optimized to approach the desired envelope in the best way.

As future work, we will compare the proposed method with other approaches for the removal of artifacts from the envelope.

## REFERENCES


[1] A. Merlo, D. Farina, and R. Merletti, "A fast and reliable technique for muscle activity detection from surface emg signals," *IEEE Transactions on Biomedical Engineering*, vol. 50, no. 3, pp. 316–323, 2003.

[2] M. Reaz, M. Hussain, and F. Mohd-Yasin, "Techniques of emg signal analysis: Detection, processing, classification, and applications," *Biological Procedures Online*, vol. 8, pp. 11–35, 2006.

[3] S. Schiaffino and C. Reggian, "Fiber types in mammalian skeletal muscles," *Physiological Review*, vol. 91, no. 4, pp. 1447–1531, Oct 2011.

[4] A. Fuglevand, D. Winter, E. Patla-Aftab, and S. Daniel, "Detection of motor unit action potentials with surface electrodes: Influence of electrode size and spacing," *Biological Cybernetics*, vol. 67, pp. 143–153, 1992.

[5] D. Farina, A. Crosetti, and R. Merletti, "A model for the generation of synthetic intramuscular emg signals to test decomposition algorithms," *IEEE Trans. Biomed. Eng*, vol. 48, no. 1, pp. 66–77, Jan 2001.

[6] A. Hamilton-Wright and D. Stashuk, "Physiologically based simulation of clinical emg signals," *IEEE Trans. Biomed. Eng.*, vol. 52, pp. 11–35, 2005.

[7] S. Kale and S. Dudul, "Intelligent noise removal from emg signal using focused time-lagged recurrent neural network," *Appl. Comp. Intell. Soft Comput.*, vol. 2009, pp. 1:1–1:9, jan 2009.

[8] S. Thongpanja, A. Phinyomark, F. Quaine, Y. Laurillau, C. Limsakul, and P. Phukpattaranont, "Probability density functions of stationary surface emg signals in noisy environments," *IEEE Trans. Inf. Theory*, vol. 63, no. 6, pp. 1547–1557, 2016.

[9] G. Tallison, P. Godfrey, and G. Robinson, "Emg signal amplitude assessment during abdominal bracing and hollowing," *Journal of Electromyography and Kinesiology*, vol. 8, pp. 51–57, 1996.

[10] L. Chen and H. Yaru, "Feature extraction and classification of ehg between pregnancy and labour group using hilbert-huang transform and extreme learning machine," *Computational and Mathematical Methods in Medicine*, vol. 2017, pp. 1–9, 02 2017.

[11] T. D'Alessio and S. Conforto, "Extraction of the envelope from surface emg signals," *IEEE Eng. Med. Biol. Mag. : the quarterly magazine of the Engineering in Medicine  Biology Society*, vol. 20, pp. 55–61, 11 2001.

[12] H. Xie and Z. Wang, "Mean frequency derived via hilbert-huang transform with application to fatigue emg signal analysis," *Computer Methods and Programs in Biomedicine*, vol. 82, p. 312320, 4 2006.

[13] G. Jang, J. Kim, S. Lee, and Y. Choi, "Emg-based continuous control scheme with simple classifier for electric-powered wheelchair," *IEEE Trans. Instrum. Elec.*, vol. 65, no. 7, pp. 3695–3705, 2016.

[14] K. Lin, X. Chen, X. Huang, Q. Ding, and X. Gao, "A hybrid bci speller based on the combination of emg envelopes and ssvep", journal="applied informatics," vol. 2, p. 1, Jan 2015.

[15] R. Kleissen and G. Zilvold, "Estimation uncertainty in ensemble average surface emg profiles during gait," *Journal of electromyography and kinesiology : official journal of the International Society of Electrophysiological Kinesiology*, vol. 4, pp. 83–94, 12 1994.

[16] G. Lehman and S. Mcgill, "The importance of normalization in the interpretation of surface electromyography: A proof of principle," *Journal of manipulative and physiological therapeutics*, vol. 22, pp. 444–6, 10 1999.

[17] Y. Chien Hung, H. Wen Vincent Young, C. Yen Wang, Y. Hung Wang, P. Lei Lee, J. Horng Kang, and M. Tzung Lo, "Quantifying spasticity with limited swinging cycles using pendulum test based on phase amplitude coupling," *IEEE Trans. Nucl. Sci*, vol. 24, pp. 1–1, 10 2016.

[18] C. Y. L. Ram rez, M. Ruano, "Analisis de bios nales:enfoquet ecnico en elan al cl nico e se nales fonocardiografisca," *Univ. Nacional de Colombia*, vol. 1, pp. 1–1, 10 2016.

[19] L. Myers, M. Lowery, M. OMalley, C. Vaughan, C. Heneghan, A. St Clair Gibson, and R. Sreenivasan, "Rectification and non-linear preprocessing of emg signals for cortico-muscular analysis," *Journal of Neuroscience Methods*, vol. 124, no. 2, p. 157165, 2003.

[20] T. J. Roberts and A. M. Gabaldón, "Interpreting muscle function from emg: lessons learned from direct measurements of muscle force." *Integrative and comparative biology*, vol. 48 2, pp. 312–20, 2008.

[21] Y. Shmaliy, "An iterative kalman-like algorithm ignoring noise and initial conditions," *IEEE Trans. Signal Process.*, vol. 59, pp. 2465 – 2473, 07 2011.

[22] Y. S. Shmaliy, F. Lehmann, S. Zhao, and C. K. Ahn, "Comparing robustness of the kalman,$h_\infty$, and ufir filters," *IEEE Trans. Signal Process.*, vol. 66, no. 13, pp. 3447–3458, 2018.

[23] L. Gila, A. Malanda, I. Rodrguez Carreo, J. Rodrguez Falces, and J. Navallas, "Electromyographic signal processing and analysis methods," *SciELO Analytics*, vol. 32, 2009.

[24] G. De Luca, *Fundamental Concepts in EMG Signal Acquisition*, 1st ed. DelSys Inc, 06 2019.

[25] J. Ives and J. K Wigglesworth, "Sampling rate effect of surface emg timing and amplitude measures," *Clinical biomechanics (Bristol, Avon)*, vol. 18, pp. 543–52, 08 2003.

[26] D. Dua and E. Karra Taniskidou, "Uci machine learning repository," *Irvine, CA: University of California, School of Information and Computer Science*, 2017.

[27] Y. S. Shmaliy, "Unbiased fir filtering of discrete-time polynomial state-space models," *IEEE Trans. Signal Process.*, vol. 57, no. 4, pp. 1241–1249, 2009.

[28] Y. Shmaliy, A. Marienko, and A. Savchuk, "Gps-based optimal kalman estimation of time error, frequency offset, and aging," 12 1999.

[29] A. E. J. Bryson and L. J. Henrikson, "Estimation using sampled data containing sequentially correlated noise." *Journal of Spacecraft and Rockets*, vol. 5, pp. 662–665, 2014.

[30] O. Aviles, J. Rodriguez, M. Herrera, and G. Martinez, "Uci machine learning repository," 2012.

[31] J. Diaz, A. Bassi, A. Coolen, E. Vivaldi, and J. Letelier, "Envelope analysis links oscillatory and arrhythmic eeg activities to two types of neuronal synchronization," *NeuroImage*, vol. 172, 02 2018.

[32] M. Jeansonne and J. Foley, "Review of the exponentially modified gaussian (emg) function since 1983," *Journal of Chromatographic Science*, vol. 29, pp. 258–266, 06 1991.

[33] A. Golubev, "Exponentially modified gaussian (emg) relevance to distributions related to cell proliferation and differentiation," *Journal of Theoretical Biology*, vol. 262, no. 2, pp. 257 – 266, 2010.

[34] S. Hall, *Basic Biomechanics*, 07 2018.

[35] M. Atzori, A. Gijsberts, C. Castellini, H. A. B. Caputo, S.Elsig, G. Giatsidis, F.Bassetto, and H. Muller, "Electromyography data for non-invasive naturally controlled robotic hand protheses," *Scientific Data 1:140053*, 2014.